Quest Journals
Journal of Electronics and Communication Engineering Research
Volume 10 ~ Issue 2 (2024) pp: 01-12
ISSN(Online) : 2321-5941
www.questjournals.org

Research Paper

Coordinated Control Scheme for Enhancing Power Quality and Managing Energy in Hybrid Renewable Energy Generation System

J.Shashank[1], K.Durga Prasad[2], G.Nikhil[3], B.Ganesh[4], M.Vinod[5]
[1,2,3,4]*(Departement of Electrical And Electronic Engineering),*[5]*(Assistant Professor - Departement of Electrical And Electronic Engineering)*
[1,2,3,4,5]*(J.B.Institute of Engineering and Technology, Hyderabad – 500075) Corresponding Author: J.Shashank*

ABSTRACT
These days, producing electricity involves using renewable energy sources like wind power systems and solar photovoltaic (PV) panels. The current and predicted weather patterns have a significant impact on these systems. Both production and fluctuations in the output are impacted by the system's inconsistent behavior. Consequently, it is becoming increasingly important for energy distribution and transmission networks to make timely adjustments. A new smart grid application for power system operation is presented in this research. To decrease undesirable harmonics, balance reactive power in the power sources, and enhance power quality and flow in the distribution system, a Static Compensator (STATCOM) device is used. A Three-Phase Four-Wire (3P4W) distribution system is connected to a quasi-Z-Source Inverter (qZSI) based STATCOM. The recommended compensator circuit used for switching in this instance consists of a PV system and a q Z-source. An Adaptive Frequency Fixed (AFF) - Second Order Generalized Integrator (SOGI) has been constructed to control the proposed compensator. Kp and Ki, two of the proportional-integral (PI) controller's parameters, are optimized using the fuzzy logic controller (FLC). The system successfully lowers the source current's Total Harmonic Distortion (THD), bringing it down from 25.5% to 1.3%, as shown by the experimental findings. Furthermore, the technology has proven that it can provide the load with active power.

INDEX TERMS *Fuzzy logic controller, harmonic distortion, power quality, quasi-Z-source inverter, renewable energy sources.*

***R**eceived 14 Feb., 2024; **R**evised 26 Feb., 2024; **A**ccepted 28 Feb., 2024 © The author(s) 2024.*
P**ublished with open access at **www.questjournals.org

I. INTRODUCTION

The development of commercially feasible alternative means of producing electrical energy is significantly hampered by the rapid global growth in environmental deterioration. As a result, enormous research efforts are being made all over the world to discover a way to provide an environmentally acceptable and long-term sustainable answer in the field of providing electric power. PV, wind farms, fuel cells, and biomass are the leading players in the industry that generates renewable energy [1]. Wind-driven stand-alone systems are a reliable energy source that has demonstrated their capacity to supply many rural clients with electricity worldwide, especially in regions with a medium to high potential for wind energy. While this is true, the oversizing of wind turbines and the requirement for an excessive amount of energy storage capacity discourage consumers from continuing with the installation of renewable energy sources in places where local circumstances are less favorable. There are many locations throughout the world where one may find plenty of solar energy, which can be paired with high or medium-high wind energy potential to reduce the requirement for energy storage in normal stand-alone systems [2].The majority of the time, independent solar and wind power consumption is unable to keep up with the grid's fluctuating demands because of these resources' significant daily availability changes.Stand-alone solar and wind energy systems need to have a large amount of storage capacity to meet the energy needs of distant customers [3]. By utilizing the complementing qualities of solar and wind power, it is feasible to lower the quantity of energy storage required in a system. It is well known that there are numerous types of distributed power production for microgrid applications. Nonetheless, the dependability of the microgrid depends on the interface power converter. Thus, the effective power regulation of the interface power converter will guarantee a stable and trustworthy distributed power generation system [4].

Therefore, the development of an off-grid quasi-Z-source inverter, a novel kind of interacting inverter, is the main focus of this study [5]. PV systems employ a range of power converter topologies, each with pros and cons of its own. Some examples include using a two-level or multilevel inverter and whether or not to use a transformer. The more conventional two-stage inverters are being replaced with single-stage inverters due to their small size, low cost, and excellent dependability [6]. On the other hand, the typical inverter needs to be larger to handle the enormous fluctuations in PV array voltage caused by the low output voltage of the PV panels and the wide range of variation dependent on temperature and irradiance, which is generally at a ratio of 1:1. The low voltage output of an inverter must be connected to the grid via huge low-frequency transformers; however, these transformers have several disadvantages, such as larger size, lower efficiency, increased acoustic noise, and higher total costs. By employing a boost DC/DC converter to raise the input voltage from a wide range to the intended constant value, the two-stage inverter does away with the requirement for a transformer [7].

The DC/DC converter turns out to be the most costly and effective part of the system because of a broken switch.

Galvanic isolation, which can be implemented on the AC output side of a line frequency transformer or in the DC/DC boost converter that uses a high-frequency transformer, is a feature of various solar-powered energy generation systems for increased safety [8]. Such additional galvanic isolations increase the overall cost and size of the system and decrease its overall efficacy. Transformer less topologies need more research because of their higher efficiency, smaller size, and lower cost for the PV system [9]. Because of its single-stage power converter for step-up and step-down operations, the qZSI has been used in PV systems [10], [11].

Furthermore, the inverter can handle a wide variety of PV DC voltage changes without being overpowered. This lowers the system's total cost, lowers the number of components and their expenses, and improves stability and dependability. PV systems may profit from several distinctive and intriguing advantages provided by qZSIs. By removing the need for additional filtering capacitors and drawing a stable current from the PV panel, the qZSI reduces switching ripples and streamlines the PV system. It also makes the PV system simpler and has a lower component rating (capacitor). This study interfaced with the PV-generating equipment using qZSI for the isolated load situation. To improve the distribution system's power quality, the study's authors describe installing an AFFSOGI control scheme in conjunction with a photovoltaic array and a qZSI-STATCOM that is backed by a Wind Energy Conversion System (WECS). The two are used in tandem to achieve this. These are the main objectives that this inquiry seeks to fulfill. Using an AFF-SOGI-based control algorithm to regulate the qZSI-STATCOM can help enhance the power quality in the distribution system when there is a DC offset in the load currents and distorted and unbalanced voltages. Thanks to the qZSI-STATCOM's multi-mode capabilities, this can be accomplished in the presence of both situations.

Here is an outline of the paper's structure. Section II contains the system configuration. Section III provides an overview of the process for system modeling and control design. In part IV, experimental research is used to validate the suggested system. Section V concludes the paper.

I. SYSTEM DESCRIPTION

Power generators, like wind turbines and photovoltaic cells, are used to supply the load more efficiently than any other power source due to their low cost and flexible operation.

As a result, both linear and non-linear loads are dependent upon the wind turbine. Compensation circuits are employed in distribution networks to enhance power quality. In tandem with the distribution network is a STATCOM compensator based on a qZSI, which addresses the power quality problems at the source. In the proposed compensator circuit, the qZSI and PV system have been merged into one, and STATCOM is used for switching. Figure 1 depicts the qZSI-based STATCOM model that has been presented. The compensator is instructed by the AFF-SOGI control approach to maintain the voltage and frequency of the wind energy system within allowable bounds. This contributes to the 3P4W distribution system's harmonic attenuation as well. The frequency controller's parameters are optimized by the fuzzy-tuned PI controller. This method balances the reactive power from the power sources and removes harmonics to regulate the flow of power to the load.

The flowchart for choosing the PV-qZSI-STATCOM operation mode is displayed in Fig. 2. With coordinated control, this PV-assisted qZSI-STATCOM operates in four distinct modes. The power electronic switches (S1– S7) are shown in four modes: Mode 1 (production of PV power), Mode 2 (battery backup), Mode 3 (continuous supply), and Mode 4 (flywheel energy storage). When the power generated by the PV power-producing system exceeds the power connected to the load (PLoad), the control system goes into mode 1. The switches in this mode are set as follows: S1, S2, S3, S4 = On (If battery's State of Charge (SOC) $\leq$ 50%), S5 = Off, S6, S7 = On. When the PV system's output of PV power declines to PPV < 10%, the control system switches to mode: 2. When Vsabc equals zero, the mode: 3 settings are activated, and the switch positions are set as follows: (S1, S2, S3 = On, S4 = On (If PPV < 10%), S5 = Off, S6, S7 = On). The control system will enter mode 4 after it has determined that the power produced by the wind energy system P wind is more than the power generated by the load PLoad. Fig. 3 shows the transition condition from one mode to another.

AFF-SOGI CONTROL FOR qZSI-STATCOM

Reactive power consumption from connected loads can be compensated for and harmonics may be reduced with the aid of the qZSI-STATCOM control, which functions to improve the power grid's dependability over time. Making the grid currents pure sinusoids at distorted load currents and imbalanced voltages is another objective. As a result, the AFF-SOGI can be used to estimate sinusoidal reference grid currents regardless of distorted load currents or imbalanced grid voltages [11], [12]. The AFF-SOGI control scheme for QZSI-STATCOM is shown in Fig. 4. Only the fundamental frequency currents are taken into account by AFF-SOGI.ZCD stands for Zero Crossing Detector, S/H for Sample and Hold Circuit, and Abs for Absolute. This is accomplished by preventing the other frequency component from creating the currents in question, preventing those currents from entering the grid and only permitting those produced by the other frequency component. As a result, the system only draws active power from the source [13], [14]. Furthermore, the controller utilizes unit voltage vectors that are calculated based on the positive sequence voltages in the grid. This guarantees that the reference currents are unaffected by distortions and imbalances in the grid voltages. By substituting fractional order versions of these numbers for the damping factor and the sonant frequency, this method—which is derived from a SOGI algorithm based on a constant frequency—allows for the extraction of the fundamental current[15], [16]. The addition of a DC offset rejection loop has greatly enhanced the AFF-SOGI. This loop guarantees that the DC offsets present in the load current no longer affect the fundamental current estimation [17]. The AFF-SOGI schematic is shown in Fig. 5, which also shows how its internal components are organized. The expression that follows may be used to define the AFF-SOGI's in-quadrature transfer function:

$$.q\,v'' = {}^{3}+(k\,1+m\,\omega\,n\,m)m\,s\,^{2}\omega + n\,(\omega\,s\,2^{2}n\,s\,)^{2}s + k\,1(\omega\,n\,)^{2} \quad (1)$$

$$\frac{v\quad s}{=} \frac{(\omega_n)}{} \quad (2)$$

$$v \quad s^{\,3+(k_1+m\omega_n)s^2+(\omega_n)^2 s+k_1(\omega_n)^2}$$

The in-quadrature fundamental-frequency signals are denoted by v ′ and q ′. m ′ and n ′ represent the fractional order damping factor and resonant frequency, respectively. The signals at the fundamental frequency are represented by v ′ and q ′ notation, respectively. The fractional order damping factor may be represented by m ′, while the resonant frequency can be represented by n ′

$$m' = -2\cos(\mu) \quad (3)$$

$$x$$

1

$$\omega_{n}' = \omega_{n} x \quad (4)$$

Overshoot and settling time during the AFF-SOGI the transient, as well as the value f ωn = 2πf rad/s, are used to calculate m. Refer to (5), the ratio μ/x can be defined as

$$\frac{}{x} = \begin{cases} \mu & \pi - \tan^{-1}\dfrac{\sqrt{4-m^2}}{m} \quad 0 < m < 2 \\ \pi & m \geq 2 \end{cases} \quad (5)$$

Although the frequency fixed (FF)-SOGI is used as a base for the AFF-SOGI, the latter is optimized concerning the parameters m and n. However, if m ′ and n ′ are adjusted with x, AFF-SOGI may become adaptable enough to handle fluctuations in grid frequency. However, the process may also be used to calculate basic load currents. The active current is calculated by holding a sample of the approximated fundamental currents at each zero crossing of the quadrature unit vectors. A ZCD is used to determine whether a signal has crossed zero. Grid voltage phase and frequency are carried in unit vectors enabling synchronization via these vectors. Since distortion and imbalanced voltages may deform vectors, they should be pure sinusoids of unit amplitude [18], [19]. The unit vectors are generated using equence voltages for this purpose. The following is a list of the phase voltagesof the grid, according to the most recent estimations available:

1

$$v_{sa} = \frac{}{3}(2v_{sabp} + v_{sabp}) \quad (6)$$

1

$$v_{sb} = \frac{}{3}(-v_{sabp} + v_{sbcp}) \quad (7)$$

1

$$v_{sc} = \frac{}{3}(-v_{sabp} - 2v_{sbcp}) \quad (8)$$

Let, vsabp, vsbcp and vscap are the positive sequence line voltages of the grid, vsa, vsb, and vsc are the grid phase voltages and the grid line voltages are denoted by vsab, vsbc, and vsca. The amplitudes of PCC voltages, VT, and unit templates in-phase and quadrature-phase are computed as follows:

$$VT = \sqrt{\left[\frac{2}{3(v_{sa}^2 + v_{sb}^2 + v_{sc}^2)}\right]} \quad (9)$$

$$U\,a = \frac{v\,s\,a}{v\,t}, u\,b = \frac{v\,s\,b}{v\,t}, u\,c = v\,s\,c/v\,t \quad (10)$$

$$Q\,a = u\,a\,/\sqrt{3} + u\,c\,/\sqrt{3} \quad (11)$$

$$Q\,b = \sqrt{3}u\,a\,/2 + (u\,b - u\,c)/2\sqrt{3} \quad (12)$$

$$Q\,b = -\sqrt{3}u\,a\,/2 + (u\,b - u\,c)/2\sqrt{3} \quad (13)$$

Let, Ua, Ub, and Uc are the in-phase unit templates and qa, qb, and qc are the quadrature-phase unit templates. When there are three phases of active currents being employed, the following equation is used to obtain the average active current:

$$I_{p\,avg} = \frac{I_{pa} + I_{pb} + I_{pc}}{3} \quad (14)$$

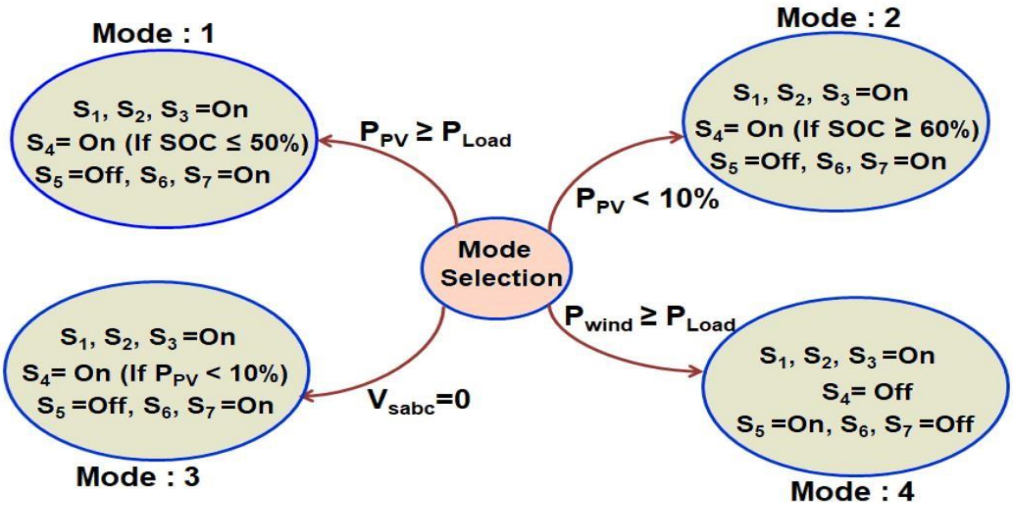

FIGURE 3. PV-assisted qZSI-STATCOM operating modes

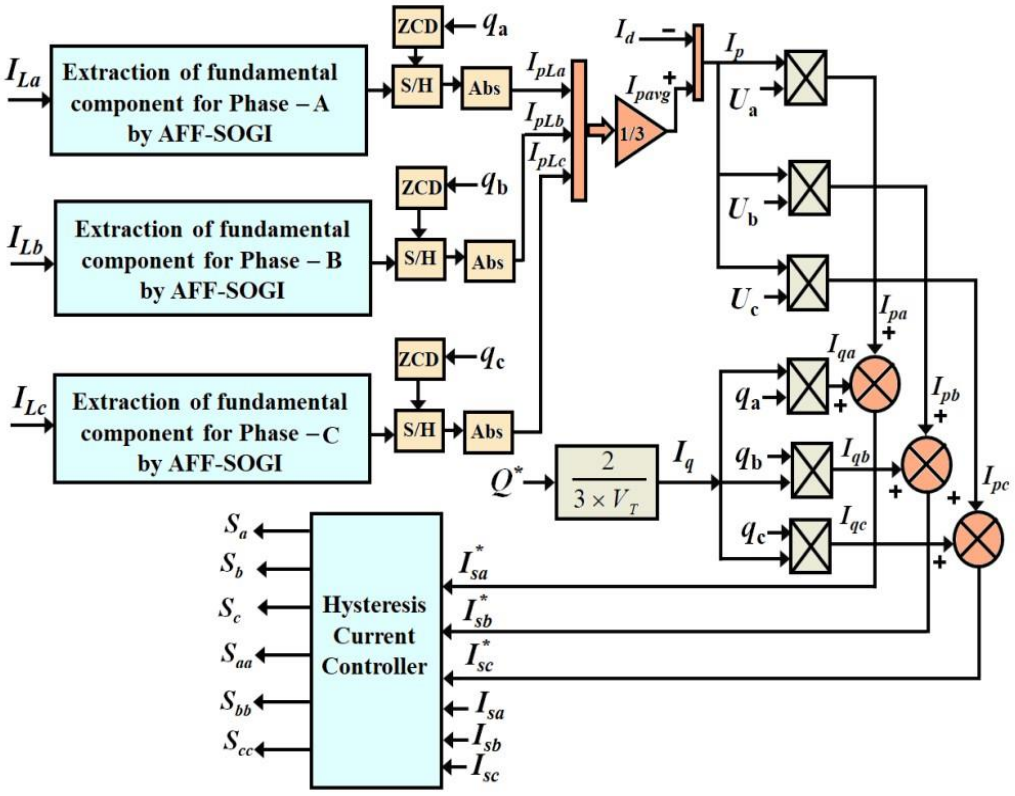

FIGURE 4. AFF-SOGI control scheme for qZSI-STATCOM.

A. FREQUENCY CONTROL

Three-phase terminal voltages are used as the input for a Phase Locked Loop (PLL), which determines the frequency of the system [20]. The estimated frequency is compared to the reference frequency using a fuzzy-tuned PI controller, which also controls the frequency error. The frequency PI controller's output is the active current that is pulled by the compensator circuitry.

$$I_d(n) = I_d(n-1) + K_{pd}\{f_{er}(n) - f_{er}(n-1)\} + K_{id} f_{er}(n) \quad (15)$$

The difference in frequency between the reference frequency of the terminal voltage (f $*$) and the measured frequency of the terminal voltage (fer(n)) is shown for each sampling instant by the formula fer(n) = f$*$ − f(n). The proportional and integral gains for the frequency PI controller are denoted by Kpd and Kid, respectively. The PI controller gain parameters are adjusted using the fuzzy-tuned PI controller. Fig. 6 depicts the fuzzy-tuned PI frequency controller. The PI controller parameters (KP and KI) should be changed at each time step k, according to equations (16) and (17).

$$K_p(k+1) = K_p(k) + \Delta K_p(k) \quad (16,17)$$

$$K_I(k+1) = K_I(k) + \Delta K_I(k)$$

Each rule table has 15 rules, and the implementation results confirm that the computing cost is within tolerable bounds. The following is the implication of their statement:

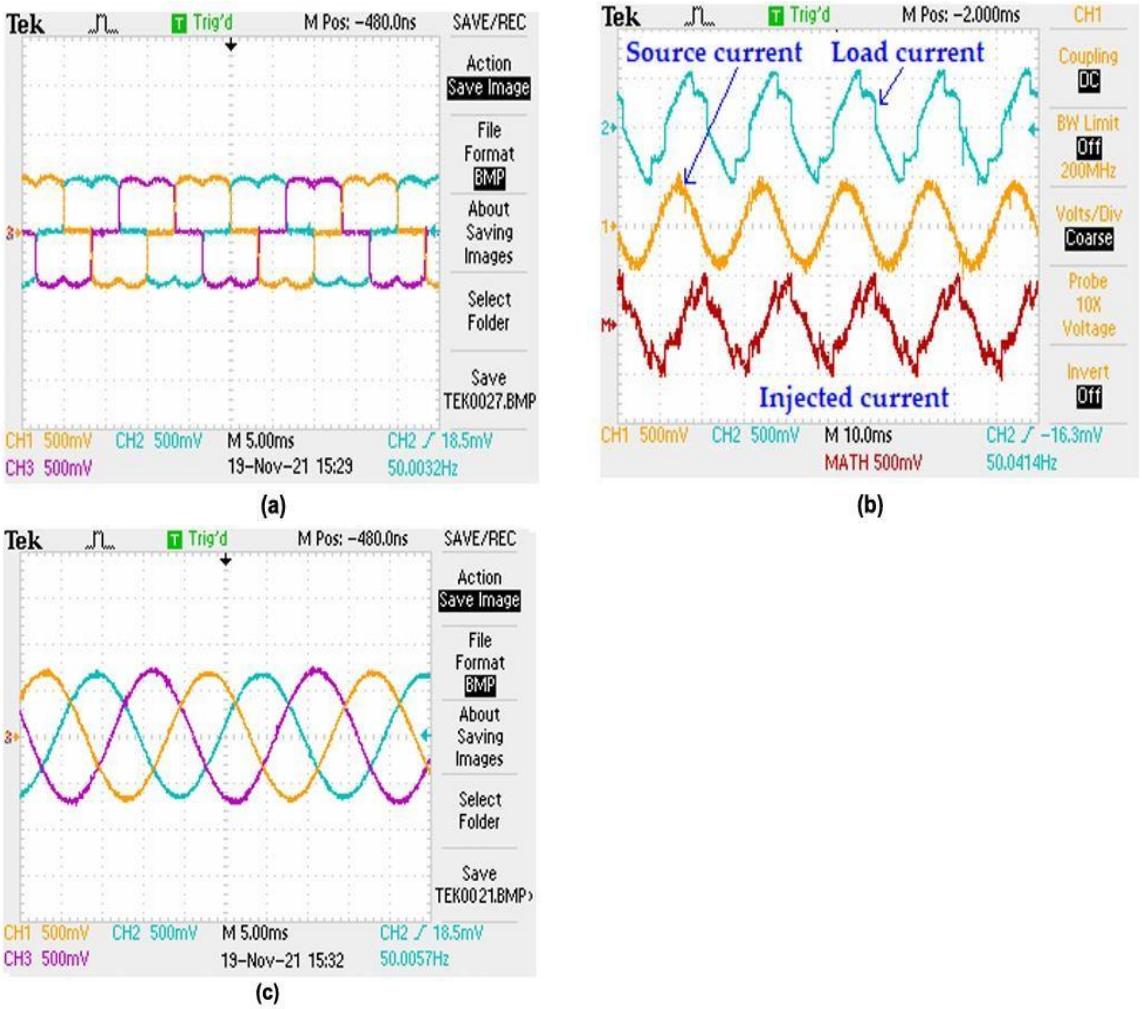

FIGURE 8. Case 1 compensation experimental results: (a) Balanced load current (ILabc) (b) Load, source, and injected current (c) Current at the source side (ISabc).

For example, if e is represented by the Ai and ec by the Bj, then KP/ KI is Cij/Dij, where the Ai, Bj, Cij, and Dij are related to the fuzzy subsets of e, ec, KP, and KI. To accomplish fuzzy inference, Mamdani's Min-Max approach is employed. Using fuzzy subsets Cij, the degree of membership for the parameter KP may be calculated as follows:

$$u_c(\Delta K_p) = \wedge^7_{i,j=1}\{[u_i(e) \wedge u_j(de)] \wedge u_{Cij}(\Delta K_p)\} \quad (18)$$

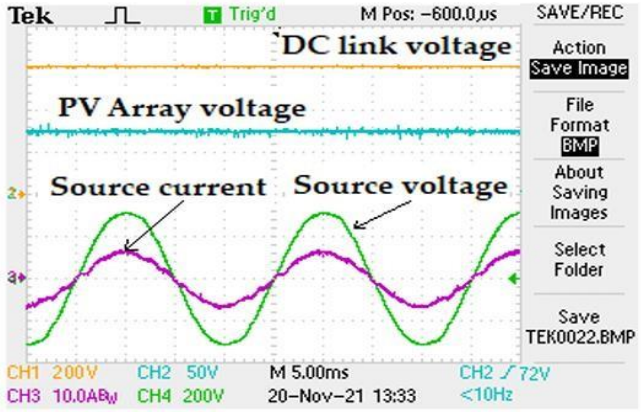

FIGURE 9. Voltage at DC link (Vdc), Voltage of PV array (VPV), and Source voltage and current.

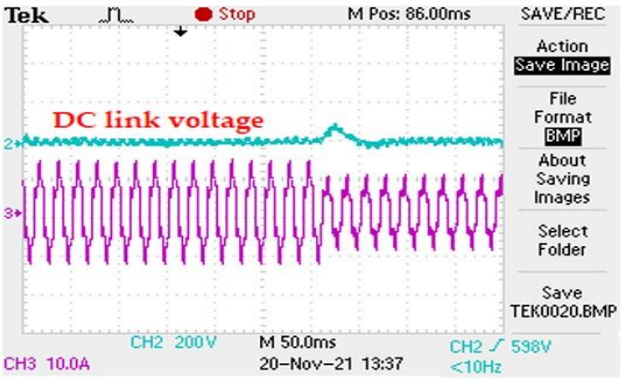

(a)

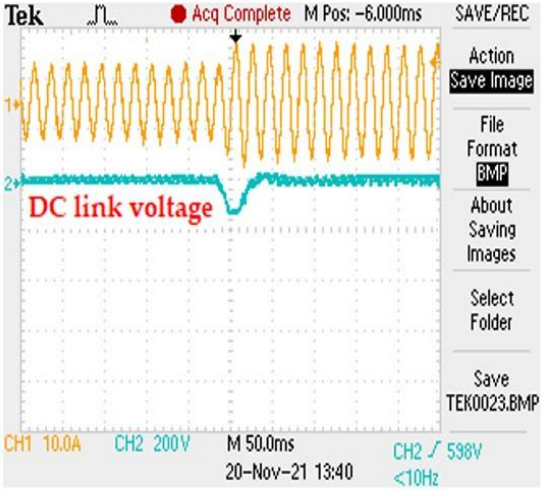

(b)

FIGURE 10. Controlling the DC -link voltage's dynamic aspects: (a) The voltage of the DC -link if the load current decreases (b) the Voltage of the DC link with a rise in load current.

The symbol u(x) represents the degree of membership. Defuzzification is the process of converting fuzzy variables into discrete values or integers in computing. The center of gravity method must be applied to obtain the clear values. The parameter KP, which is equivalent to KI, may be found using following equation:

$$\Delta K_p(e, de) = \frac{\sum_{k=1}^{7} \Delta K_p u_c(\Delta K_p)}{\sum_{k=1}^{7} u_c(\Delta K_p)} \quad (19)$$

B. ESTIMATION OF REFERENCE CURRENT

Average active currents result in evenly distributed three-phase load requirements. Grid currents are always balanced as a result, regardless of voltage imbalance or uneven load demand. The following formula is used to get the reference grid current's total active current:

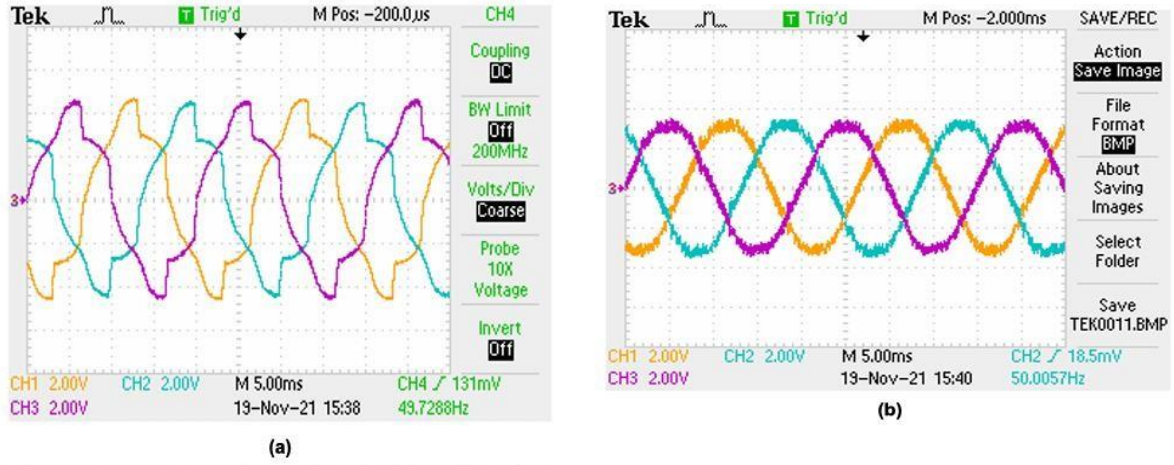

FIGURE 11. Experimental results of (a) Uncompensated current and (b) Compensated source current.

Calculating the required current to maintain the DC-link voltage requires the following Equation:

Vdce represents the difference between the observed and referenced DC-link voltages, and the variables kpd and kid represent the proportional and integral gains of the PI controller. Referring to eq.(22), the reactive current of the reference grid can be estimated as follows.

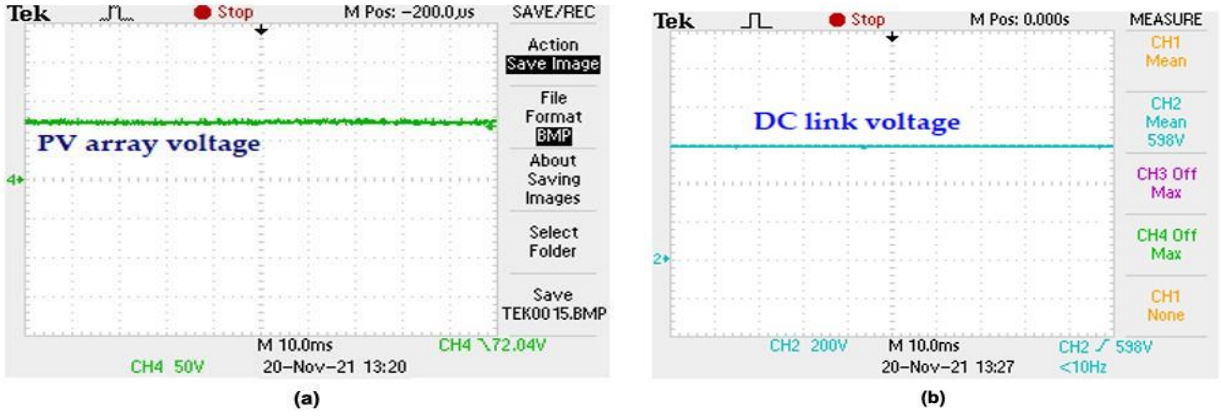

FIGURE 12. (a) PV array voltage (b) DC link voltage.

For grid reactive power correction, $Q*$ is the amount of reactive power that needs to be generated. These are the approximate values for the grid's active and reactive reference currents.

$Ipa = Ip \times Ua, Ipb = Ip \times Ub, Ipc = Ip \times Uc$ (20)

$Iqa = Iq \times qa, Iqb = Iq \times qb, Iqc = Iq \times qc$ (21)

As a result, we may derive the grid's reference currents as follows:

$I* sa = Ipa + Iqa, I* sb = Ipb + Iqb, I* sc = Ipc \times Iqc$ (22)

A comparison is made between the grid reference currents and the measured grid currents. The hysteresis current controller generates the ON/OFF switching patterns for the IGBT gate driving signals. Therefore, the grid current errors are calculated.

$Isa\ er = I* sa - Isa, Isb\ er = I* sb - Isb, Isc\ er = I* sc - Isc$ (23)

These grid current error signals are amplified and then compared with a triangle carrier wave in the hysteresis current controller, which results in the generation of switching pulses for the qZSI-STATCOM.

II. EXPERIMENTAL VALIDATION

Using an experimental prototype, the output of the PV-aided STATCOM with AFF-SOGI controller is tested under various load conditions. In each of the situations, the system's feasibility was evaluated. Below are several case studies illustrating the results of experimental prototypes. The system parameters used in the experiment are listed in Table 1.

TABLE 1. System parameters used for the experiment.

Symbol	Value	Description
V_{ph}	230V	System Voltage (Phase)
f	50Hz	System Frequency
L	26 mH	Filter Inductance
R	1.5Ω	Resistance
Ah	500Ah	battery capacity
PV_w	600 W	Power output of PV array
V_{PV}	72V	PV Nominal voltage
V_L / V_{Ph}	400 V/ 230 V	SEIG Voltage
P	4 kW	SEIG Power rating
N	1410 rpm	SEIG speed
kW	10 kW	Flywheel rated power
N_f	1500 rpm	Flywheel speed
D_f	500 mm	Diameter of Flywheel

A. CASE 1: BALANCED NON-LINEAR LOADS AT CONSTANT WIND SPEED

PV-STATCOM is assessed when the wind speed is maintained constant and non-linear loads are balanced. The current compensation experimental results for Case 1 compensation are displayed, as Fig. 8 makes clear. The compensator circuit can be used to keep the voltage and current constant even when the non-linear balanced load has an impact.

Fig. 9 displays the experimental findings for the DC link voltage, PV array voltage, source voltage, and current.

The dynamic characteristics of DC-link voltage regulation can be assessed by changing the load current. Figure 10(a) depicts the DC-link voltage when the load current is increased, and Figure 10(b) shows the DC-link voltage when the load current is dropped. When the load current increases, the DC link voltage reduces, and vice versa when the load current decreases.

The harmonic spectrum for the uncompensated source current is shown in Fig. 11. The integration of the qZSISTATCOM reduces the THD for compensated source current from 25.6%, 25.4%, and 25.5% to 1.3%, 1.4%, and
1.3%, respectively, as shown in Fig. 12.

B. CASE 2: BALANCED LOAD CURRENT WITH VARYING WIND SPEED

It shows that the grid current becomes sinusoidal and stays in phase with the phase voltage as soon as the qZSISTATCOM is turned on. This usually leads to an operation with a power factor of unity. Uncompensated load current and compensated source current with compensator circuitry are shown in Fig. 11.

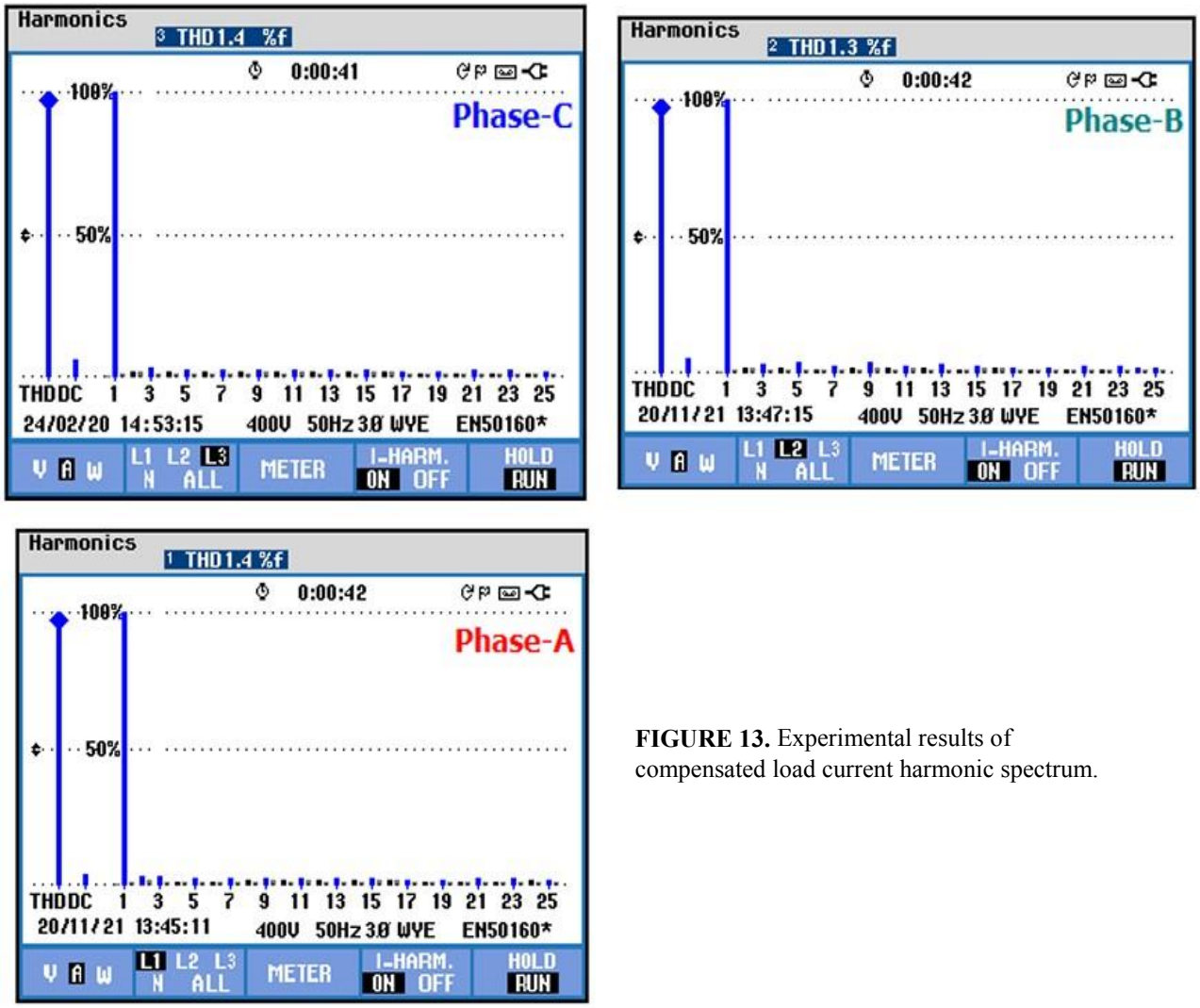

FIGURE 13. Experimental results of compensated load current harmonic spectrum.

Fig. 12 displays the DC-link voltage and PV array voltage of the qZSI-based PV-STATCOM. Figures 13 respectively, show the source current's THD both before and after adjustment. It has been observed that following adjustment, the source current's THD decreases from 25.2%, 25.4%, and 25.5% to 1.3%, 1.4%, and 1.3%, respectively. Because of this, STATCOM, which is based on AFF-SOGI, can effectively correct the load current's harmonics even in situations when the wind speed varies.

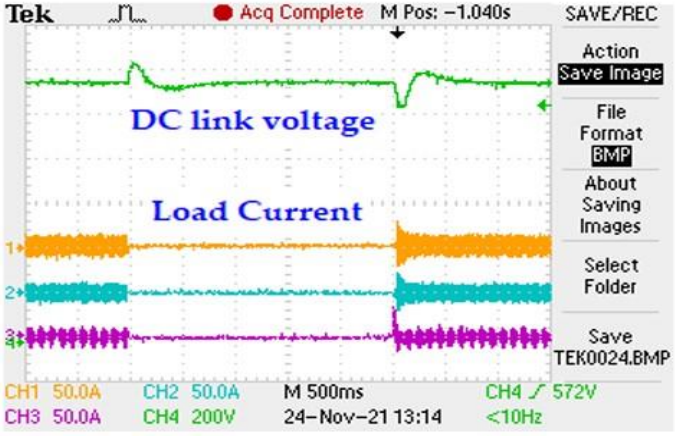

FIGURE 14. DC link voltage during step load changes.

C. CASE 3: UNBALANCED LOAD CURRENTS WITH VARYING WIND SPEED

The QZSI-STATCOM, which is based on the AFF-SOGI, can supply a sinusoidal source current with a THD of less than 2% and no DC offset. Fig. 17 displays the source voltage and current as well as the uncompensated load current. The compensator circuitry is included in the measurements of the source current and voltage, respectively.

Figures 13 respectively, show the source current's THD both before and after correction. It has been observed that following adjustment, the source current's THD decreases from 25.5%, 25.7%, and 25.4% to 1.4%, 1.3%, and 1.4%, respectively. Because of this, even in cases where the load current is unbalanced, STATCOM, which is based on AFF-SOGI, can effectively compensate for the harmonics of the load current.

The outcomes of applying step loads are displayed in Fig. 14. Actual power that was previously supplied is moved to the DC link when a nonlinear load is switched off, pending the determination of a new supply current reference that is suitable for the new load current.

The DC link voltage so rises above the reference value. There is a 50V drop in the DC link voltage when the nonlinear load is switched. In both cases, the DC connection voltage stabilizes after a few power cycles. Table 2 displays the THD analysis of several case studies for the suggested controller. It is found that the THD is only 1.3%, which is significantly less than the IEEE-519 recommended maximum limit of 5% [23]. This suggests that the controller can maintain a distortion-free sinusoidal grid current even in the presence of distorted grid voltage and load current. These smooth unit templates offer distortion-free reference grid currents that have allowed for THD content. To enhance the filtering capacity without introducing any additional latency, it is possible to incorporate two parallel filter loops dedicated to dominant harmonic components alongside the primary loop.

TABLE 2. THD of load and source current of the proposed system.

Case study	THD of Load current (%)			THD of Source current (%)		
	I_{La}	I_{Lb}	I_{Lc}	I_{Sa}	I_{Sa}	I_{Sa}
1	25.6	25.4	25.5	1.3	1.4	1.3
2	25.2	25.4	25.5	1.3	1.4	1.3
3	25.5	25.7	25.4	1.4	1.3	1.4

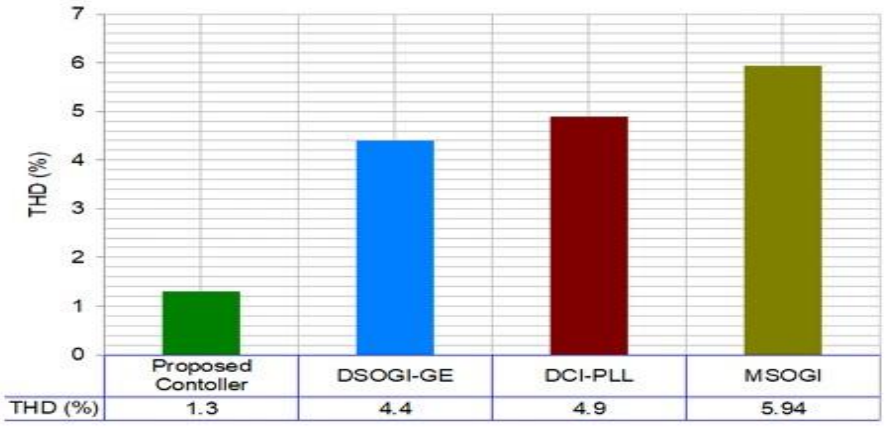

FIGURE 15. THD comparison of AFF-SOGI with a different controller.

Parameters	Proposed Work	Popavath et al. 2018[24]	Ahmed et al. 2019[25]	Kumar et al. 2020 [26]
Type of System	Grid Integrated	Grid Integrated	Grid Integrated	Grid Integrated
RES	Wind+PV+ Battery	Wind+PV	PV+Battery	Wind+Battery
Compensator device	qZSI-STATCOM	VSC-STATCOM	VSC-STATCOM	VSC-STATCOM
Controller	AFF-SOGI	Instantaneous reactive power theory	SRF Theory	SRF Theory
THD(%) of source current	1.3	5.0	2.26	2.72

TABLE 3. THD results for different topologies and controllers.

The results of the THDsoftheAFF-SOGI are contrasted in Fig. 15 with those of several other controllers that are currently available in the literature and are thought to be state-of-the-art.

The Double Second-Order Generalized Integrator-Gradient Estimator (DSOGI-GE), DC-Immune PLL (DCIPLL), and Modified SOGI (MSOGI), proposed by Patil et al. 2017 [14], were the other three controllers selected for comparison with the proposed AFF-SOGI. Through simulation studies, the suggested system is evaluated using the MATLAB/Simulink program. Table 3 presents a comparison between the results obtained from this investigation and those reported in previous similar research studies. It is evident that the grid-integrated hybrid PV-SEIG wind energy system that is being offered, along with qZSI STATCOM help, either outperforms many existing hybrid RES system schemes or reaches performance levels comparable to those that have been documented in published studies.

III. CONCLUSION

Major players in the power industry acknowledge the significant contribution FACTS has made to raising the quality of the power system. Furthermore, the integration of qZSI-STATCOM devices with renewable energy plants can be achieved because of the STATCOM devices' capabilities. These qualities include improving voltage trips, power flow management, and transient stability—all of which are necessary for the functioning of wind and solar power facilities. Climate in the surrounding area has a significant impact on these systems.

The system's erratic behavior has an impact on the range of output and production values. Consequently, a new smart grid application has been created to be used in power system management to control power flow, increase capacities, reduce distribution system harmonics, and correct power source-induced voltage disruptions. The method that is provided allows the performance of the qZSI STATCOM to be improved when the fuzzy-tuned PI controller is utilized to make adjustments.

Consequently, a new smart grid application has been created to be used in power system management to control power flow, increase capacities, reduce distribution system harmonics, and correct power source-induced voltage disruptions. The method that is provided allows the performance of the qZSI STATCOM to be improved when the fuzzy-tuned PI controller is utilized to make adjustments.

REFERENCES

[1] L. de Oliveira-Assis, P. García-Triviño, E. P. P. Soares-Ramos, R. Sarrias-Mena, C. A. García-Vázquez, C. E. Ugalde-Loo, and L. M. Fernández-Ramírez, ‘‘Optimal energy management system using biogeography based optimization for grid-connected MVDC microgrid with photovoltaic, hydrogen system, electric vehicles and Zsource converters,’’ Energy Convers. Manage., vol. 248, Nov. 2021, Art. no. 114808, doi: 10.1016/j.enconman.2021.114808.

[2] S. Ouchen, A. Betka, S. Abdeddaim, and A. Menadi, ‘‘Fuzzy-predictive direct power control implementation of a grid-connected photovoltaic system, associated with an active power filter,’’ Energy Convers. Manage., vol. 122, pp. 515–525, Aug. 2016, doi: 10.1016/j.enconman.2016.06.018. [3] P. Aree, ‘‘Dynamic performance of selfexcited induction generator with electronic load controller under starting of induction motor load,’’ in Proc. 5th Int. Conf. Electr., Electron. Inf. Eng. (ICEEIE), Malang, Indonesia, Oct. 2017, pp. 21–24, doi: 10.1109/ICEEIE.2017.8328756.

[4] A. B. Shitole, H. M. Suryawanshi, G. G. Talapur, S. Sathyan, M. S. Ballal, V. B. Borghate, M. R. Ramteke, and M. A. Chaudhari, ‘‘Grid interfaced distributed generation system with modified current control loop using adaptive synchronization technique,’’ IEEE Trans. Ind. Informat., vol. 13, no. 5, pp. 2634–2644, Oct. 2017, doi: 10.1109/TII.2017.2665477.

[5] H. Abu-Rub, A. Iqbal, S. M. Ahmed, F. Z. Peng, Y. Li, and G. Baoming, ‘‘Quasi-Z-source inverter-based photovoltaic generation system with maximum power tracking control using ANFIS,’’ IEEE Trans. Sustain. Energy, vol. 4, no. 1, pp. 11–20, Jan. 2013, doi: 10.1109/TSTE.2012.2196059.

[6] J.Zhang, ‘‘Unified control of Z-source grid-connected photovoltaic system with reactive power compensation and harmonics restraint: Design and application,’’ IET Renew. Power Gener., vol. 12, no. 4, pp. 422–429, Mar. 2018, doi: 10.1049/iet-rpg.2016.0478.

[7] J. G. Cintron-Rivera, Y. Li, S. Jiang, and F. Z. Peng, ‘‘Quasi-Z source inverter with energy storage for photovoltaic power generation systems,’’ in Proc. 26th Annu. IEEE Appl. Power Electron. Conf. Expo. (APEC), Fort Worth, TX, USA, Mar. 2011, pp. 401–406, doi: 10.1109/APEC.2011.5744628.

[8] N. Cheraghi Shirazi, A. Jannesari, and P. Torkzadeh, ‘‘Self-start-up fully integrated DC–DC step-up converter using body biasing technique for energy harvesting applications,’’ AEU-Int. J. Electron. Commun., vol. 95, pp. 24–35, Oct. 2018, doi: 10.1016/j.aeue.2018.07.033.

[9] S. Parthiban and V. Madhaiyan, ‘‘Experimental validation of solar PV sustained ZSI based unified active power filter for enrichment of power quality,’’ Automatika, vol. 62, no. 1, pp. 137–153, Jan. 2021, doi: 10.1080/00051144.2021.1908013.

[10] M. Vijayakumar and S. Vijayan, ‘‘PV based three-level NPC shunt active power filter with extended reference current generation method,’’ Int. J. Electr. Energy, vol. 2, no. 4, pp. 258–267, 2014, doi: 10.12720/ijoee.2.4.258267.

[11] M. Vijayakumar and S. Vijayan, ‘‘A novel reference current generation method of PV based three-level NPC shunt active power filter,’’ UPB Sci. Bull. C, vol. 77, no. 3, pp. 235–250, 2015.

[12] A. K. K. Giri, S. R. Arya, R. Maurya, and B. C. Babu, ‘‘Power quality improvement in stand-alone SEIGbased distributed generation system using Lorentzian norm adaptive filter,’’ IEEE Trans. Ind. Appl., vol. 54, no. 5, pp. 5256–5266, Sep. 2018, doi: 10.1109/TIA.2018.2812867.

[13] M. Ahmed, M. Orabi, S. Ghoneim, M. Alharthi, F. Salem, B. Alamri, and S. Mekhilef, ‘‘Selective harmonic elimination method for unequal DC sources of multilevel inverters,’’ Automatika, vol. 60, no. 4, pp. 378–384, Oct. 2019, doi: 10.1080/00051144.2019.1621048.

[14] K. Patil and H. H. Patel, ‘‘Modified SOGI based shunt active power filter to tackle various grid voltage abnormalities,’’ Eng. Sci. Technol., Int. J., vol. 20, no. 5, pp. 1466–1474, Oct. 2017, doi: 10.1016/j.jestch.2017.10.004.

[15] B. Singh, S. Kumar, and C. Jain, ‘‘Damped-SOGI-based control algorithm for solar PV power generating system,’’ IEEE Trans. Ind. Appl., vol. 53, no. 3, pp. 1780–1788, May/Jun. 2017, doi: 10.1109/TIA.2017.2677358. [16] J. A. Barrado, R. Grino, and H. Valderrama-Blavi, ‘‘Power-quality improvement of a stand-alone induction generator using a STATCOM with battery energy storage system,’’ IEEE Trans. Power Del., vol. 25, no. 4, pp. 2734–2741, Oct. 2010, doi: 10.1109/TPWRD.2010.2051565.

[17] F. U. Nazir, N. Kumar, B. C. Pal, B. Singh, and B. K. Panigrahi, ‘‘Enhanced SOGI controller for weak grid integrated solar PV system,’’ IEEE Trans. Energy Convers., vol. 35, no. 3, pp. 1208–1217, Sep. 2020, doi: 10.1109/TEC.2020.2990866.

[18] S. Senguttuvan and M. Vijayakumar, ‘‘Solar photovoltaic system inter-faced shunt active power filter for enhancement of power quality in the three-phase distribution system,’’ J. Circuits, Syst. Comput., vol. 27, no. 11, Oct. 2018, Art. no. 1850166, doi: 10.1142/S0218126618501669.

[19] T. Jayakumar and A. A. Stonier, ‘‘Implementation of solar PV system unified ZSI-based dynamic voltage restorer with U-SOGI control scheme for power quality improvement,’’ Automatika, vol. 61, no. 3, pp. 371–387, Jul. 2020, doi: 10.1080/00051144.2020.1760591.

[20] M. Ghanaatian and S. Lotfifard, ‘‘Control of flywheel energy storage systems in the presence of uncertainties,’’ IEEE Trans. Sustain. Energy, vol. 10, no. 1, pp. 36–45, Jan. 2019, doi: 10.1109/TSTE.2018.2822281.

[21] K. Muthuvel and M. Vijayakumar, ‘‘Solar PV sustained quasi Z-source network-based unified power quality conditioner for enhancement of power quality,’’ Energies, vol. 13, no. 10, p. 2657, May 2020, doi: 10.3390/en13102657.

[22] M. Hanif, M. Basu, and K. Gaughan, ‘‘Understanding the operation of a Z-source inverter for photovoltaic application with a design example,’’ IET Power Electron., vol. 4, no. 3, pp. 278–287, 2011, doi: 10.1049/iet pel.2009.0176.

[23] IEEE Recommended Practice and Requirements for Harmonic Control in Electric Power Systems, IEEE Standard 519-2014 (Revision of IEEE Std 519-1992), 2014, pp. 1–29, doi: 10.1109/IEEESTD.2014.6826459. [24] F. S. Ahmed, A. N. Hussain, and A. J. Ali, ‘‘Power quality improvement by using multiple sources of PV and battery for DSTATCOM based on coordinated design,’’ IOP Conf. Ser., Mater. Sci. Eng., vol. 745, no. 1, Feb. 2020, Art. no. 012025, doi: 10.1088/1757-899X/745/1/012025.

[25] L. Popavath and P. Kaliannan, ‘‘Photovoltaic-STATCOM with low voltage ride through strategy and power quality enhancement in a grid integrated wind-PV system,’’ Electronics, vol. 7, no. 4, p. 51, Apr. 2018, doi: 10.3390/electronics7040051.

[26] L. Ashok Kumar and V. Indragandhi, ‘‘Power quality improvement of grid-connected wind energy system using facts devices,’’ Int. J. Ambient Energy, vol. 41, no. 6, pp. 631–640, May 2020, doi: 10.1080/01430750.2018.1484801.